

## Research Article

# Construction of small Zn-air batteries by dendrite-free Zn electrodeposition using renewable electricity

Vasiliki Premeti<sup>1</sup>, Maria Katsaiti<sup>1</sup>, Evangelos Papadogiannis<sup>1</sup>, Vassilios Dracopoulos<sup>2</sup>, Panagiotis Lianos<sup>1\*</sup>

<sup>1</sup>Department of Chemical Engineering, University of Patras, 26500 Patras, Greece

<sup>2</sup>FORTH/ICE-HT, P.O. Box 1414, 26504 Patras, Greece

E-mail: lianos@upatras.gr

**Received:** 26 July 2023; **Revised:** 8 September 2023; **Accepted:** 11 September 2023

**Abstract:** In this work, the possibility to make small, handy but efficient Zn-air batteries has been studied. Battery anode has been constructed by dendrite-free Zn electrodeposition on conductive substrates made of either carbon cloth or brass. Brass was an alloy containing 71% Cu and 21% Zn. Zn electrodeposition has been monitored by applying several (negative) electric potentials ranging between 0 and  $-0.5$  V. Dendrite-free deposits were obtained for voltages ranging between 0 and  $-0.2$  V while extensive dendrite formation was observed with voltages equal to  $-0.5$  V. Uniform Zn deposits were obtained by using the brass substrate. Zn electrodeposition could be realized with a renewable electricity source, in particular by using a photocatalytic fuel cell or a photovoltaic cell. The substrate (electrode) with deposited Zn film was subsequently employed as anode electrode in a Zn-air battery and the battery characteristics have been monitored. The procedures followed in this work support solar energy conversion and storage in a Zn-air battery.

**Keywords:** Zn-air batteries; Zn electrodeposition; dendrite-free electrodeposition; brass substrate; carbon cloth substrate

## 1. Introduction

Zn-air batteries are a promising technology for energy storage and release. They are based on a simple construction involving a Zn anode, an air cathode and a (usually) alkaline electrolyte [1,2]. There are many advantages associated with this type of batteries: they depend on Zn, which is abundant in the earth's crust, therefore, they are not expensive; they carry an aqueous electrolyte, therefore, they are environmentally benign and they have a high theoretical energy density of  $1086 \text{ W h kg}^{-1}$  and specific capacity of  $820 \text{ A h kg}^{-1}$ . In addition, they are rechargeable, in the sense that Zn metal is consumed during battery discharging and produced during battery charging. Details on Zn-air battery charge-discharge operation as well as recent challenges faced by their commercialization can be found in many recently published works [1–14].

In the present work, we have studied the construction of small Zn-air batteries by simple procedures based on the use of renewable electricity for Zn electrodeposition on common electrodes and have also studied battery operation and its power storage and yield. Larger batteries can be always made by upgrading; however, small batteries may find applications in electronic devices with small energy demand, for example hearing aids [14]. Particular attention has been presently paid to the conditions of Zn electrodeposition by avoiding dendrite formation [15–27]. Dendrite formation is one serious reason for fast battery deterioration. When a Zn-air battery is charged, Zn metal is deposited on the anode electrode. This may lead to dendrite formation. Several

Copyright ©2023 Vasiliki Premeti, et al.

DOI: <https://doi.org/10.37256/2220233443>

This is an open-access article distributed under a CC BY license

(Creative Commons Attribution 4.0 International License)

<https://creativecommons.org/licenses/by/4.0/>

procedures have been adopted to avoid such a formation. Notably, several researchers have regulated dendrite-free Zn deposition by paying attention to the composition of the electrolyte [17, 20, 26] or by exploiting the magnetodynamic effect during Zn deposition [16]. Brass [15] and a Zn-Sn alloy [19] have been used as preferable substrates for dendrite-free metallic Zn deposition while other researchers relied on the beneficial presence of carbon nanostructures to assure the same effect [21–24]. Finally, 3D printing is a handy method for Zn electrode construction and appropriate inks have been developed for dendrite-free Zn deposition [25]. The question of dendrite formation is not limited to Zn but it is a matter that concerns as well the popular Li-based batteries [27]. Herein, we have adopted these published procedures to make Zn electrodes by choosing the most easy and simple approach. More specifically, carbon cloth and technical grade brass have been employed as electrodes for anodic Zn electrodeposition by using an external source of electricity. The use of carbon cloth or similar materials provides the additional advantage of making flexible batteries. Particular attention has been paid to the employment of renewable energy resources such as a photocatalytic fuel cell (PFC) and a silicon photovoltaic cell.

## 2. Materials and methods

### 2.1 Materials

All reagents used in the present work were from Sigma-Aldrich unless otherwise indicated. Thus, Zn foil, 1.6 mm thick, 99% metal basis, was from Alfa Aesar, carbon cloth (CC) from Fuel Cell Earth and carbon black (CB) from Cabot Corporation (Vulcan XC72). Brass foil, 2 mm thick, was a commercial technical grade alloy. Energy Dispersive X-ray spectroscopy (EDX) analysis showed that it was made of 71% Cu and 29% Zn.

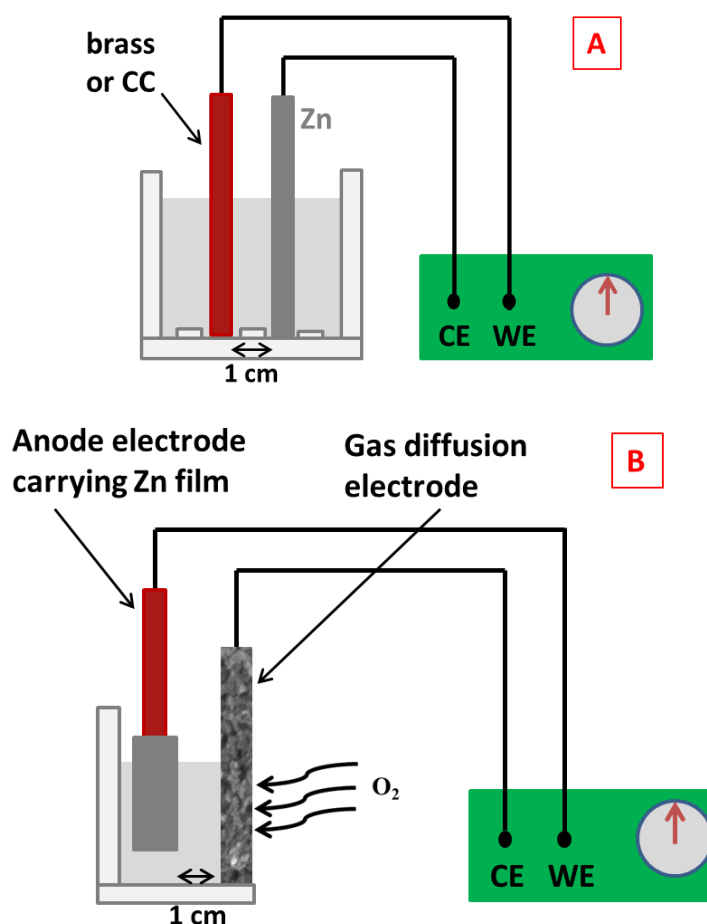


**Figure 1.** Schematic illustration of the reactor for Zn electrodeposition (A) and Zn-air battery operation (B)

### 2.2 Deposition of Zn on CC or Brass

Carbon cloth or brass electrodes of dimension 3 cm × 1 cm have been used as substrates to electrochemically deposit a Zn film. A rectangular reactor made of Plexiglas has been used in all cases (see Figure 1A). CC or brass electrodes were used as working electrode while a Zn foil of similar geometry was used as counter electrode. Both working and counter electrodes were immersed in an aqueous electrolyte made of 5 M KOH containing 0.2 M ZnO. The solubility of Zn salts and ZnO in an alkaline electrolyte is very limited; therefore, only a tiny quantity of ZnO or, for example, Zn acetate can be introduced in the solution but it suffices for the present application. The working electrode was immersed by 1.2 cm in the electrolyte; therefore, the total area in contact with the liquid phase was approximately 2.4 cm<sup>2</sup>, i.e., both sides immersed. The distance between the electrodes was 1 cm in all cases. Electrodeposition of metal Zn was obtained under potentiostatic conditions at various voltages ranging from 0 to -0.5 V. In some cases, the electric power was provided by either a photoelectrochemical cell or a photovoltaic cell (see section 3.2). All electrodes were carefully weighed dry before and after deposition. Drying of the electrodes was assured by placing them for a few minutes in an oven at 100 °C. After electrodeposition, a film was formed on both sides of the electrode, covering all immersed surface. Such electrodes with deposited Zn film were employed as Zn anodes for the construction of Zn-air batteries. Characterization of the Zn films was made with Field Emission Scanning Electron Microscopy (FESEM) and EDX using a Zeiss SUPRA 35VP system (Germany) and X ray diffraction (XRD) with a Bruker D8 Advance diffractometer.

### 2.3 Construction and operation of Zn-air batteries

A second reactor, also made of Plexiglas has been used to construct and study Zn-air batteries (*cf.* Figure 1B). The CC or brass electrode with deposited Zn film was used as anode electrode while a carbon cloth loaded with carbon black (CB/CC) was used as air-diffusion cathode. Deposition of CB was made on only one side of the CC electrode by using a paste made of 300 mg CB and 100 mg PTFE as binder mixed in 10 ml water or isopropanol. By using a laboratory mixer working at high speed, a viscous paste was obtained which was easily spread on the CC electrode with a spatula. The film was annealed at 340 °C. The covered side of the CC was in contact with the electrolyte while the other side was exposed to the air. The hydrophobic layer of CB prevented water (electrolyte) leak. The electrolyte was the same as in section 2.2, i.e., an aqueous electrolyte of 5 M KOH containing 0.2 M ZnO. The anode was immersed in the electrolyte by 1 cm, i.e., the total area in contact with the electrolyte was 2 cm<sup>2</sup>. The active area of the gas-diffusion electrode was 1 cm<sup>2</sup>. All measurements were made with the help of an Autolab potentiostat PGSTAT128N (Utrecht, The Netherlands).

## 3. Results and discussion

### 3.1 Characterization of the electrodeposited Zn films

In section 2.2, it was said that Zn films can be electrodeposited on working electrodes made either of CC or brass. Other substrates may be also used for the same purpose but have not been examined in this work. The quantity of deposited material is a function of deposition time and applied electric bias. For reasons of uniformity, all data in this work correspond to a standard deposition time of 30 min. Table 1 shows the quantity of deposited Zn for various values of applied electric potential. As expected, the quantity of the deposited Zn increased with the strength of the negative bias and of the corresponding current. At positive potentials, no Zn is deposited on the working electrode. This is expected, since only the negative voltage attracts Zn<sup>2+</sup> ions present in solution and reduces them leading to metal Zn deposition. At zero potential, a very small quantity of Zn was deposited. The source of deposited Zn is the counter Zn electrode. This can be easily verified since it was repeatedly found that the Zn electrode loses mass during operation approximately equal to the quantity of the deposited mass. If instead of Zn, another material is used as counter electrode, for example, carbon or stainless steel, no measurable quantity of Zn is deposited. The quantity of Zn in solution (0.2 M) is too small to substitute for the Zn electrode source. For reasons of uniformity and basic control, the Zn electrode was equal in size and geometry with the CC or the brass electrode. However, any Zn source will suffice to supply the necessary quantity of Zn, independent of geometry or size.

**Table 1.** Quantity of deposited Zn on CC or brass electrodes for a standard deposition time of 30 min

Potential (V)	Electrode	Current (mA)	Mass# (mg)	Electrode	Current (mA)	Mass# (mg)
0	CC	-	1.5	Brass	-	1.0

-0.1	CC	-42	32.1 (25.6)	Brass	31	21.3 (18.9)
-0.2	CC	-71	54.2 (43.3)	Brass	65	45.4 (39.7)
-0.5	CC	-131	89.7 (79.8)	Brass	209	190 (128)

#The numbers in parentheses are the corresponding calculated values of mass for 100% Faradaic efficiency

Table 1 gives the values of the current flowing through the reactor during Zn electrodeposition. The theoretical quantity of Zn mass which is expected to be deposited by 100% Faradaic efficiency can be calculated using the Faraday constant,  $F = 96\,485.33 \text{ s A mol}^{-1}$ , the fact that it takes 2 electrons to reduce one  $\text{Zn}^{2+}$  cation and the atomic weight (AW) of Zn, i.e.,  $65.38 \text{ g mol}^{-1}$ . Therefore, the theoretical mass can be calculated by the following formula [2]:

$$m(\text{mg}) = \frac{I(\text{mA})xt(s)x(\text{AW})}{2xF} \quad (1)$$

which is reduced to

$$m(\text{mg}) = 0.000339xI(\text{mA})xt(s) \quad (2)$$

in the case of Zn. The calculated mass values are shown in Table 1 in parentheses. Interestingly, the calculated mass was in all cases smaller than the actual mass deposited. From one point of view, this demonstrates a very efficient electrodeposition process. The additional mass, may come from adsorbed potassium from the electrolyte or from partial transformation of Zn metal to ZnO, even though, as it will be shown here below, the percentage of potassium and oxygen was found very small by EDX spectroscopy. Deposition of debris of various origins might account for the rest.

The electrodeposited Zn films were characterized by FESEM and EDX spectroscopy. In all studied cases, the film consisted of Zn while a small quantity of oxygen and equally small quantity of K has been detected. Potassium, of course, originates from the electrolyte while the small quantity of oxygen indicates that the extent of deposited ZnO or oxide produced by exposure to the atmosphere was also limited. This result has been verified by XRD, an example of which is shown in Figure 2 showing the predominant presence of zinc in metal form.

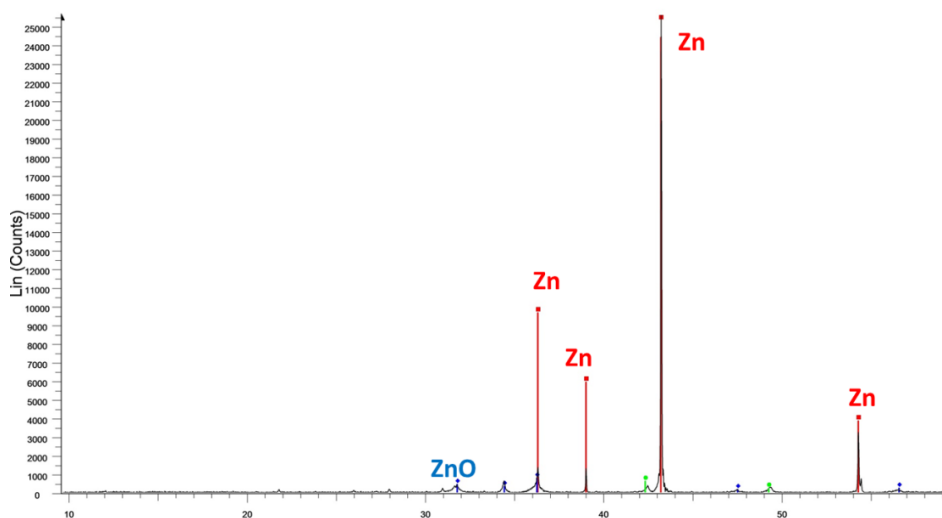


**Figure 2.** XRD spectrum for a film made by Zn electrodeposition on a brass electrode at  $-0.2 \text{ V}$  (JCPDS card Nos: Zn 03-065-3358; ZnO 01-079-2205)

Figure 3 shows FESEM images of electrodeposited Zn films on carbon cloth electrodes at various electric potentials. At  $0 \text{ V}$ , as also seen in Table 1, because of the negligible quantity of deposited Zn, the corresponding image shows only the carbon cloth filaments. As the negative potential increased, so did the quantity of Zn. The important conclusion to draw from Figure 3 is that when the potential was  $-0.5 \text{ V}$  a clear dendrite formation was observed both at low and high magnification. For intermediate potentials, not shown, a hybrid situation has been observed so that a potential of  $-0.2 \text{ V}$  is a safe limit for avoiding dendrite formation.

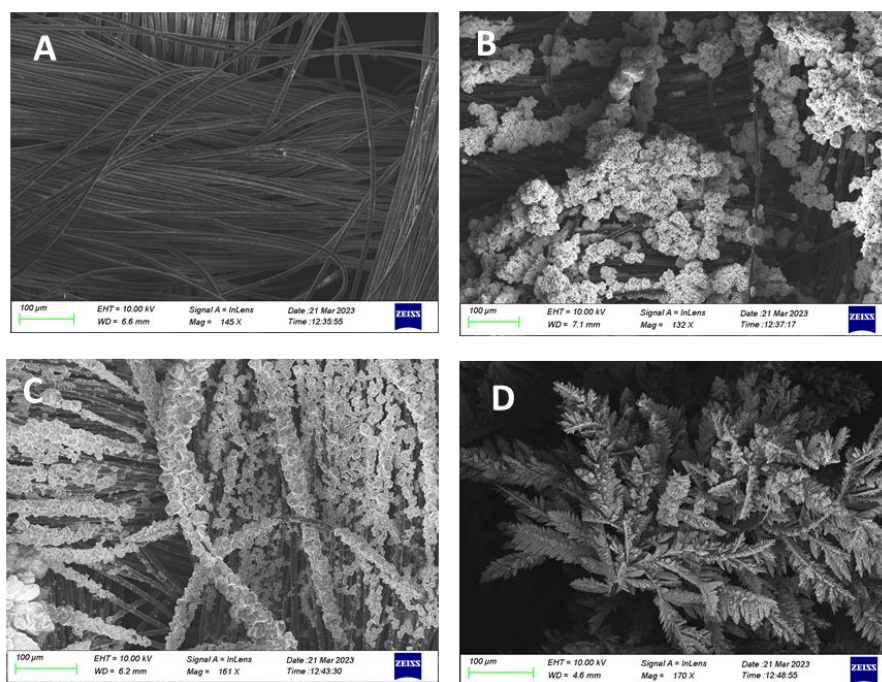


**Figure 1.** FESEM images of Zn films electrodeposited on carbon cloth electrodes at various electric potentials (Volts): (A) 0.0; (B)  $-0.1$ ; (C)  $-0.2$  and (D)  $-0.5$ . The scale bar is  $100\ \mu\text{m}$  in all cases

Dendrite-free Zn electrodeposition on carbon filaments, of course, under the condition of moderate potentials, is in line with previous findings of Zn deposition on defective carbon surface [22] and Turing membrane [23].

Zn film formation was smoother in the case of brass substrates. The brass used in the present work, as already said in section 2.1, was a commercial alloy of technical grade, which was found by EDX to be composed of 71% Cu and 29% Zn. Formation of Zn film was negligible at 0 bias but grew with increasing negative potential (and current). In the case of  $-0.5\ \text{V}$ , the film grew fast and became very voluminous. Figure 4 shows the corresponding FESEM images. Once more, it was found that with an electric potential of  $-0.5\ \text{V}$ , dendrites were formed but they were not present for potentials up to  $-0.2\ \text{V}$ . Especially in the case of  $-0.1\ \text{V}$ , a uniform and smooth Zn film has been formed, smoothly covering brass electrode over the whole surface immersed in the electrolyte. It has been previously found [15] that brass substrate makes such uniform non dendritic films and the present data verify the previous finding. It is concluded that by using brass substrates and moderate electric potential a uniform dendrite-free Zn film may be formed and may be preferably applicable to the construction of small Zn-air batteries, as analyzed below. The markedly large mass deposition and extensive dendrite formation at  $V = -0.5\ \text{V}$  is obviously responsible also for the formation of a voluminous film in that case.

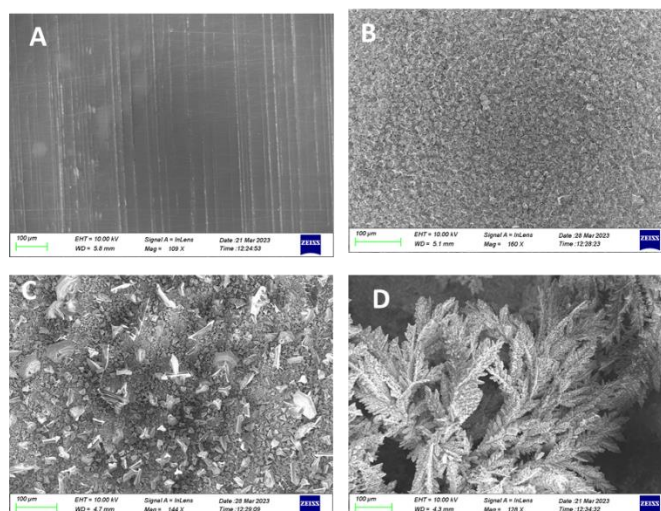


**Figure 4.** FESEM images of Zn films electrodeposited on brass electrodes at various electric potentials (Volts): (A) 0.0; (B) -0.1; (C) -0.2 and (D) -0.5. The scale bar is 100  $\mu\text{m}$  in all cases

### 3.2 Deposition of Zn on brass by using renewable electricity

Renewable electricity may be used to deposit Zn on brass (or CC or other electrode). This possibility has been presently demonstrated by using a Photocatalytic fuel cell (PFC) [2, 28, 29] as a device that converts solar radiation into electricity. A PFC is a photoelectrochemical cell composed of a photoanode carrying a photocatalyst and an air cathode functioning by oxygen reduction. In the present case the photocatalyst was a combination of mesoporous titania sensitized in the Visible by nanoparticulate CdS. As fuel, ethanol was added in the electrolyte, which was an aqueous solution of 1 M NaOH. In order to study Zn deposition, the combination of devices illustrated in Figure 5A has been used. The connection of the PFC with the electrodes of the Zn-deposition-reactor (*cf.* Figure 1A) is designed in such a way that leads photogenerated electrons to the brass electrode. A potentiostat was accordingly connected to monitor the process. Illumination of the photoanode was obtained with the help of a solar simulator. First, the functionality of the whole installation has been checked by recording a current-voltage profile, which is shown in Figure 5B. The IV curve was plotted in a light-chopping mode, in order to highlight the conditions of photocurrent production. It is seen that the photocurrent increased fast for voltages beyond  $-0.9\text{V}$ . At  $-0.2\text{V}$ , the current was approximately in a plateau of about 2.2 mA. This is a relatively small current (*cf.* Table 1) but *is pure photocurrent and it is obtained without any additional bias*. In other words, it suffices to sign light on the PFC to automatically put the system into operation. The measuring device that interferes in the system of Figure 5A is only for monitoring and may be taken out without affecting operation. The above system was indeed used to deposit Zn on a brass electrode. For reasons of uniformity, the operation lasted 30 min and deposition was affected potentiostatically at  $-0.2\text{V}$ . Because of the small current (2.2 mA), the quantity of deposited Zn on the brass substrate was only 2.5 mg. Of course, this quantity may be increased if a more powerful PFC or a photovoltaic cell is instead used. By substituting the above PFC with a commercial (small) photovoltaic cell (*cf.* graphical abstract), it was again possible to electro-deposit Zn on a brass electrode. The presently used PV cell produced a current of 26 mA potentiostatically at  $-0.2\text{V}$ . The quantity of deposited Zn was in that case 20 mg. It is then possible to deposit Zn on brass (or other electrodes) by using solar energy and any device that converts it into electricity.

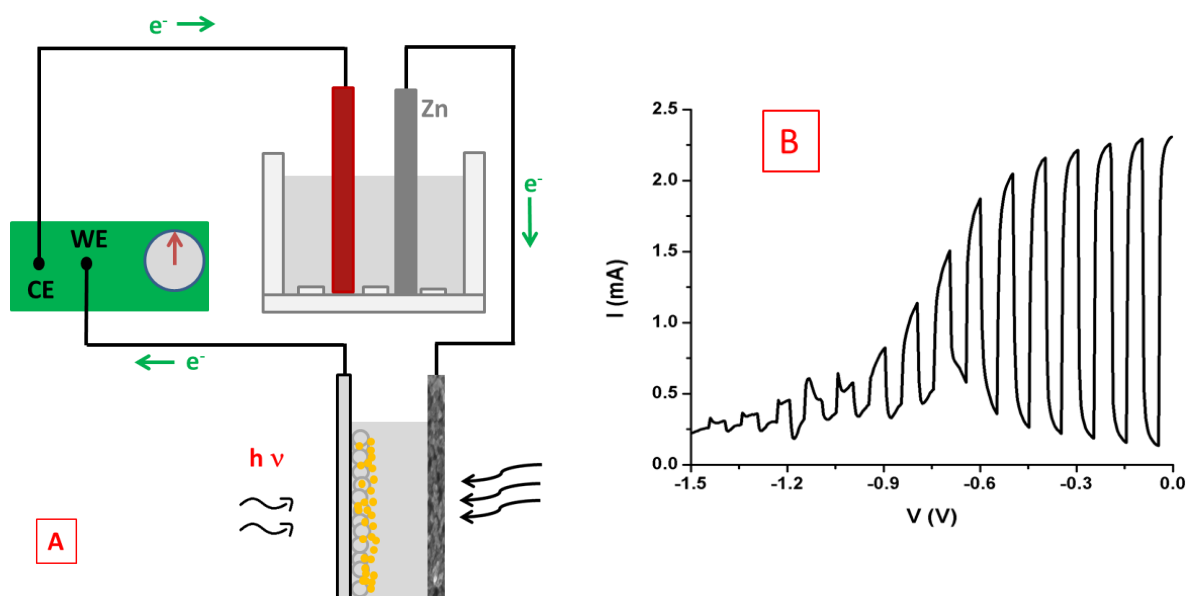


**Figure 5.** (A) Schematic illustration of the devices used and their connection for photoelectrochemical Zn deposition. (B) Corresponding current-voltage profile recorded in the light-chopping mode

### 3.3 Construction and operation of Zn-air batteries

A battery has been constructed according to the plan of Figure 1B by using as anode the optimized brass electrode, i.e., the one which carried 35.4 mg of Zn and was made at  $-0.2\text{V}$  (*cf.* Table 1). This battery had the characteristics of Figure 6A, which were similar with those of Zn-air batteries made by using a commercial Zn foil as anode [2]. Interestingly, despite of the fact that the air electrode carried only carbon black, i.e., did not carry a powerful electrocatalyst, the battery demonstrated a satisfactory performance with relatively high short-

circuit current (262 mA) and a satisfactory open-circuit voltage (1.27 V). Galvanostatic operation of the battery for several minutes at 10 mA and 100 mA gave the curves of Figure 6B. Some interesting information may be calculated out of these plots.

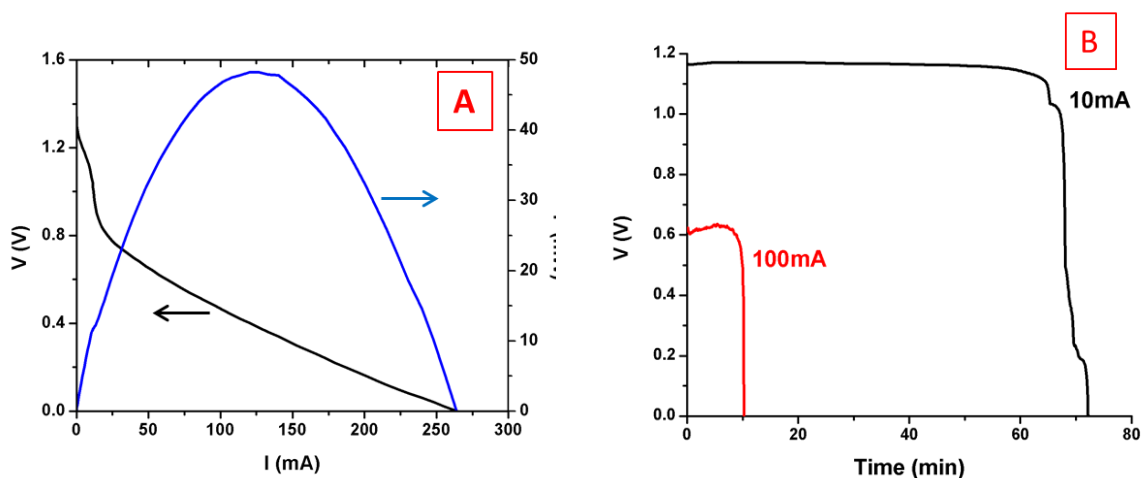


**Figure 6.** (A) V-I and P-I characteristics and (B) galvanostatic operation of a battery made by using a Zn film deposited on brass at -0.2 V as anode and a CB/CC air cathode

The energy delivered by the battery when operated at 10 mA, can be calculated by integrating the 10 mA curve in Figure 6B, i.e. by calculating the area below the curve, which directly gives the energy produced by the battery in Joules. It was found to be 49.7 J or 0.0138 W h. The quantity of Zn which was consumed during this operation was 17 mg. Therefore, the corresponding energy density is 812 W h kg<sup>-1</sup>. Since the theoretical energy density for Zn-air batteries is 1086 W h kg<sup>-1</sup>, the present battery delivered approximately 75% of its theoretical capacity, which is a very satisfactory score. When the battery functioned at 100 mA, the delivered energy was 40.9 J or 0.0114 W h. The consumed mass of Zn in that case was 30 mg; therefore, the energy density was 380 W h kg<sup>-1</sup> and its efficiency was only 35%. It is true that the lower the current the higher the efficiency of these batteries (*cf.* Ref.[2]).

## 4. Conclusions

Zn films can be deposited on various electrodes by electrodeposition and by using Zn as metal source. The electric power necessary for this operation may directly come from a renewable source, for example, solar energy.

The novelty of the present approach is that a handy battery can be made providing flexibility and easiness of construction. In addition, deposition of Zn on carbon cloth or other non-rigid electrodes has the advantage of making flexible batteries.

Dendrites may be formed during Zn deposition; however, dendrite formation can be avoided if moderate electric potentials are applied while a brass substrate favors dendrite-free and uniform film deposition.

An efficient Zn-air battery can be made by using anode electrodes made of Zn deposited on brass electrodes. This type of electrodes can be used in handy battery constructions.

In view of the fact that renewable energy can be used to deposit Zn, the whole approach corresponds to a practical renewable energy conversion and storage.

## Conflict of interest

There is no conflict of interest for this study.

## References

- [1] Li, Y.; Dai, H. Recent advances in zinc–air batteries, *Chem. Soc. Rev.*, 2014, 43, 5257-5275.
- [2] Katsaiti, M.; Papadogiannis, E.; Dracopoulos, V.; Keramidias, A.; Lianos, P. Solar charging of a Zn-air battery. *J. Power Sources* **2023**, 555, <https://doi.org/10.1016/j.jpowsour.2022.232384>.
- [3] Sun, J.; Wang, N.; Qiu, Z.; Xing, L.; Du, L. Recent Progress of Non-Noble Metal Catalysts for Oxygen Electrode in Zn-Air Batteries: A Mini Review. *Catalysts* **2022**, 12, 843, <https://doi.org/10.3390/catal12080843>.
- [4] Lu, Q.; Zou, X.; Bu, Y.; Shao, Z. Structural design of supported electrocatalysts for rechargeable Zn–air batteries. *Energy Storage Mater.* **2023**, 55, 166–192, <https://doi.org/10.1016/j.ensm.2022.11.046>.
- [5] Song, D.; Hu, C.; Gao, Z.; Yang, B.; Li, Q.; Zhan, X.; Tong, X.; Tian, J. Metal–Organic Frameworks (MOFs) Derived Materials Used in Zn–Air Battery, *Materials* 2022, 15, 5837.
- [6] Lv, X.; Chen, M.; Kimura, H.; Du, W.; Yang, X. Biomass-Derived Carbon Materials for the Electrode of Metal–Air Batteries. *Int. J. Mol. Sci.* **2023**, 24, 3713, <https://doi.org/10.3390/ijms24043713>.
- [7] Wu, W.-F.; Yan, X.; Zhan, Y. Recent progress of electrolytes and electrocatalysts in neutral aqueous zinc-air batteries. *Chem. Eng. J.* **2023**, 451, <https://doi.org/10.1016/j.cej.2022.138608>.
- [8] Samad, S.A.; Fang, Z.; Shi, P.; Zhu, J.; Lu, C.; Su, Y.; Zhuang, X. Porous carbon nanosheets for oxygen reduction reaction and Zn-air batteries, *2D Mater.*, 2023, 10, 022001.
- [9] Iqbal, A.; El-Kadri, O.M.; Hamdan, N.M. Insights into rechargeable Zn-air batteries for future advancements in energy storing technology. *J. Energy Storage* **2023**, 62, <https://doi.org/10.1016/j.est.2023.106926>.
- [10] Ola, O.; Wang, N.; Walker, G.; Zhu, Y.; Grant, D. Engineering the next generation of photorechargeable zinc-air batteries. *Curr. Opin. Electrochem.* **2022**, 35, <https://doi.org/10.1016/j.coelec.2022.101040>.
- [11] Das, S.; Kundu, A.; Kuila, T.; Murmu, N.C. Recent advancements on designing transition metal-based carbon-supported single atom catalysts for oxygen electrocatalysis: Miles to go for sustainable Zn-air batteries. *Energy Storage Mater.* **2023**, 61, <https://doi.org/10.1016/j.ensm.2023.102890>.
- [12] Kundu, A.; Mallick, S.; Ghora, S.; Raj, C.R. Advanced Oxygen Electrocatalyst for Air-Breathing Electrode in Zn-Air Batteries. *ACS Appl. Mater. Interfaces* **2021**, 13, 40172–40199, <https://doi.org/10.1021/acsami.1c08462>.
- [13] Kundu, A.; Samanta, A.; Raj, C.R. Hierarchical Hollow MOF-Derived Bamboo-like N-doped Carbon Nanotube-Encapsulated Co<sub>0.25</sub>Ni<sub>0.75</sub> Alloy: An Efficient Bifunctional Oxygen Electrocatalyst for Zinc–Air Battery, *ACS Appl. Mater. Interfaces*, 2021, 13, 30486–30496
- [14] Fu, J.; Paul Cano, Z.; Gyu Park, M.; Yu, A.; Fowler, M.; Chen, Z. Electrically Rechargeable Zinc–Air Batteries: Progress, Challenges, and Perspectives, *Adv. Mater.*, 2017, 29, 1604685
- [15] Nagy, T.; Nagy, L.; Erdélyi, Z.; Baradács, E.; Deák, G.; Zsuga, M.; Kéki, S. “In Situ” Formation of Zn Anode from Bimetallic Cu-Zn Alloy (Brass) for Dendrite-Free Operation of Zn-Air Rechargeable Battery. *Batteries* **2022**, 8, 212, <https://doi.org/10.3390/batteries8110212>.
- [16] Peng, Y.; Lai, C.; Zhang, M.; Liu, X.; Yin, Y.; Li, Y.; Wu, Z. Zn–Sn alloy anode with repressible dendrite grown and meliorative corrosion resistance for Zn-air battery. *J. Power Sources* **2022**, 526, 231173, <https://doi.org/10.1016/j.jpowsour.2022.231173>.
- [17] Liang, P.; Li, Q.; Chen, L.; Tang, Z.; Li, Z.; Wang, Y.; Tang, Y.; Han, C.; Lan, Z.; Zhi, C.; et al. The magnetohydrodynamic effect enables a dendrite-free Zn anode in alkaline electrolytes. *J. Mater. Chem. A* **2022**, 10, 11971–11979, <https://doi.org/10.1039/d2ta02077g>.
- [18] Liu, Q.; Ou, X.; Li, L.; Wang, X.; Wen, J.; Zhou, Y.; Yan, F. Recyclable and CO<sub>2</sub>-retardant Zn–air batteries based on CO<sub>2</sub>-decorated highly conductive cellulose electrolytes, *J. Mater. Chem. A*, 2022, 10, 12235.
- [19] Hui, X.; Zhang, P.; Li, J.; Zhao, D.; Li, Z.; Zhang, Z.; Wang, C.; Wang, R.; Yin, L. In Situ Integrating Highly Ionic Conductive LDH-Array@PVA Gel Electrolyte and MXene/Zn Anode for Dendrite-Free High-Performance Flexible Zn–Air Batteries, *Adv. Energy Mater.*, 2022, 12, 2201393.
- [20] Li, H.; Guo, J.; Mao, Y.; Wang, G.; Liu, J.; Xu, Y.; Wu, Z.; Mei, Z.; Li, W.; He, Y.; et al. Regulation of Released Alkali from Gel Polymer Electrolyte in Quasi-Solid State Zn–Air Battery. *Small* **2023**, 19, e2206814, <https://doi.org/10.1002/sml.202206814>.
- [21] Zhao, H.; Chi, Z.; Zhang, Q.; Kong, D.; Li, L.; Guo, Z.; Wang, L. Dendrite-free Zn anodes enabled by Sn-Cu bimetal/rGO functional protective layer for aqueous Zn-based batteries. *Appl. Surf. Sci.* **2023**, 613, <https://doi.org/10.1016/j.apsusc.2022.156129>.
- [22] Lee, J.-H.; Kim, R.; Kim, S.; Heo, J.; Kwon, H.; Yang, J.H.; Kim, H.-T. Dendrite-free Zn electrodeposition triggered by interatomic orbital hybridization of Zn and single vacancy carbon defects for aqueous Zn-based flow batteries. *Energy Environ. Sci.* **2020**, 13, 2839–2848, <https://doi.org/10.1039/d0ee00723d>.
- [23] Wu, J.; Yuan, C.; Li, T.; Yuan, Z.; Zhang, H.; Li, X. Dendrite-Free Zinc-Based Battery with High Areal Capacity via the Region-Induced Deposition Effect of Turing Membrane. *J. Am. Chem. Soc.* **2021**, 143, 13135–13144, <https://doi.org/10.1021/jacs.1c04317>.



- [24] Zeng, Y.; Zhang, X.; Qin, R.; Liu, X.; Fang, P.; Zheng, D.; Tong, Y.; Lu, X. Dendrite-Free Zinc Deposition Induced by Multifunctional CNT Frameworks for Stable Flexible Zn-Ion Batteries. *Adv. Mater.* **2019**, *31*, e1903675, <https://doi.org/10.1002/adma.201903675>.
- [25] Zeng, L.; He, J.; Yang, C.; Luo, D.; Yu, H.; He, H.; Zhang, C. Direct 3D printing of stress-released Zn powder anodes toward flexible dendrite-free Zn batteries. *Energy Storage Mater.* **2023**, *54*, 469–477, <https://doi.org/10.1016/j.ensm.2022.10.061>.
- [26] Mou, C.; Bai, Y.; Zhao, C.; Wang, G.; Ren, Y.; Liu, Y.; Wu, X.; Wang, H.; Sun, Y. Construction of a self-supported dendrite-free zinc anode for high-performance zinc–air batteries. *Inorg. Chem. Front.* **2023**, *10*, 3082–3090, <https://doi.org/10.1039/d3qi00279a>.
- [27] Liang, Y.; Ding, W.; Yao, B.; Zheng, F.; Smirnova, A.; Gu, Z. Mediating Lithium Plating/Stripping by Constructing 3D Au@Cu Pentagonal Pyramid Array. *Batteries* **2023**, *9*, 279, <https://doi.org/10.3390/batteries9050279>.
- [28] Andrade, T.S.; Dracopoulos, V.; Keramidas, A.; Pereira, M.C.; Lianos, P. Charging a vanadium redox battery with a photo(catalytic) fuel cell. *Sol. Energy Mater. Sol. Cells* **2020**, *221*, 110889, <https://doi.org/10.1016/j.solmat.2020.110889>.
- [29] Sfaelou, S.; Sygellou, L.; Dracopoulos, V.; Travlos, A.; Lianos, P. Effect of the Nature of Cadmium Salts on the Effectiveness of CdS SILAR Deposition and Its Consequences on the Performance of Sensitized Solar Cells. *J. Phys. Chem. C* **2014**, *118*, 22873–22880, <https://doi.org/10.1021/jp505787z>.